Chemical Science

ROYAL SOCIETY OF CHEMISTRY

EDGE ARTICLE

View Article Online
View Journal | View Issue

Cite this: *Chem. Sci.*, 2022, **13**, 4088

All publication charges for this article have been paid for by the Royal Society of Chemistry

Received 4th February 2022
Accepted 10th March 2022

DOI: 10.1039/d2sc00748g

rsc.li/chemical-science

Thioether-enabled palladium-catalyzed atroposelective C–H olefination for N–C and C–C axial chirality†

Yanjun Li,‡[a] Yan-Cheng Liou,‡[a] Xinran Chen‡[ab] and Lutz Ackermann *[a]

Thioethers allowed for highly atroposelective C–H olefinations by a palladium/chiral phosphoric acid catalytic system under ambient air. Both N–C and C–C axial chiral (hetero)biaryls were successfully constructed, leading to a broad range of axially chiral *N*-aryl indoles and biaryls with excellent enantioselectivities up to 99% ee. Experimental and computational studies were conducted to unravel the walking mode for the atroposelective C–H olefination. A plausible chiral induction model for the enantioselectivity-determining step was established by detailed DFT calculations.

Introduction

Axially chiral compounds are ubiquitous structural motifs in biologically active natural products,[1] privileged catalysts,[2] chiral ligands[3] and material sciences.[4] In recent years, transition-metal-catalyzed asymmetric C–H activation[5] has become an efficient and powerful synthesis platform to construct diverse axial chirality.[6,7] Atroposelective *ortho*-C–H functionalization of (hetero)biaryl precursors is one of the attractive approaches to diversified chiral (hetero)biaryls.[8] Based on this approach, numerous directing groups (DGs) have been identified to provide the required steric congestion and reactivity (Scheme 1a).[9–15] For example, isoquinolines and pyridines were employed in rhodium-catalyzed C–H functionalization for axially chiral biaryl compounds synthesis by Murai,[9] You,[10a] and Lassaletta.[11] Pyridine *N*-oxides were applied to palladium-catalyzed asymmetric C–H iodination by You.[10b] Chiral sulfoxides as DGs were elegantly utilized for diastereoselective C–H activation by Wencel-Delord/Colobert.[12] In contrast, phosphine-based DGs enabled palladium-catalyzed C–H olefinations to prepare chiral phosphineolefin compounds.[13] The Shi group found free amines[14a,b] and quinolines[14c] as efficient DGs for synthesizing axially chiral biaryl compounds *via* palladium/chiral phosphoric acid (CPA) catalytic system. Likewise, Shi group developed the atroposelective C–H functionalizations of biaryl aldehydes to prepare axially chiral aldehydes through chiral transient directing groups (cTDGs) strategy.[15] Despite these significant advances in the synthesis of axially chiral compounds, the exploration of other DGs and catalytic systems to expand more structurally diverse axially chiral biaryls continue to be in high demand.

N–C axial chirality is the key element of atropisomeric natural products and chiral catalysts,[16,17] and unexplored compared with C–C axial chirality and remains a major challenge.[18] This is largely due to the increased distance between the *ortho*-substituents next to the N–C chiral axis, leading to relatively low rotational barrier and atropostability.[18d] Recent representative contributions for the construction of N–C axially chiral scaffolds hail from the Wencel-Delord/Colobert,[19] Xie,[20]

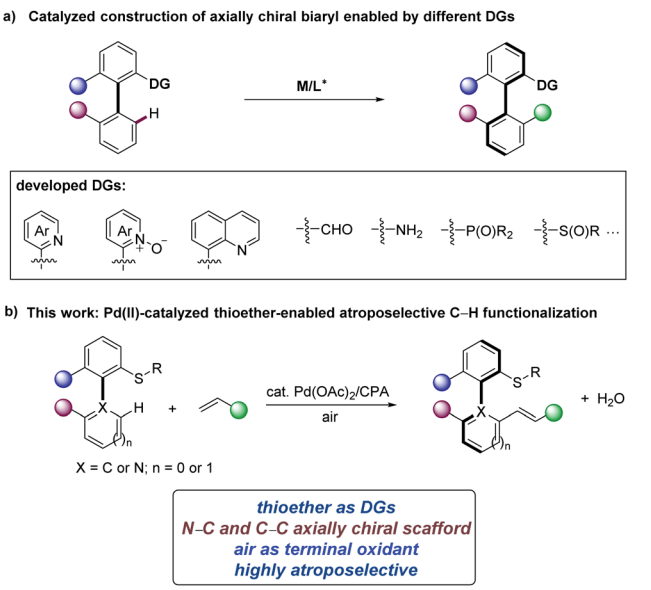

Scheme 1 Atroposelective C–H activation for axial chirality.

[a]*Institut für Organische und Biomolekulare Chemie, Georg-August-Universität Göttingen, Tammannstraße 2, 37077 Göttingen, Germany. E-mail: Lutz.Ackermann@chemie.uni-goettingen.de*

[b]*Department of Chemistry, Zhejiang University Hangzhou, 310027, China*

† Electronic supplementary information (ESI) available: Experimental details and characterization of all new compounds and details of DFT calculations. CCDC 2144688 and 2130699. For ESI and crystallographic data in CIF or other electronic format see DOI: 10.1039/d2sc00748g

‡ These authors contributed equally to this work.

Shi,[21] among others.[22] Asymmetric C–H functionalization of *N*-aryl heterocycles or *N*-aryl amides is a useful synthetic strategy to construct N–C axial chirality.[20,21,22a,g] However, this strategy was thus far unfortunately restricted to the use of super-stoichiometric amounts of cost-intensive silver salts, jeopardizing the inherent atom-economy of the C–H activation strategy.

Recently, aryl alkyl thioethers have been reported as DGs for C–H functionalization.[23] However, the use of thioethers as DGs in asymmetric C–H activation has remained elusive.[24] Within our program on sustainable C–H activation,[25] we have now unravelled a thioether-directed strategy for the enantioselective synthesis of N–C and C–C axially chiral molecules with air as the oxidant, thereby only giving H_2O as the sole byproduct (Scheme 1b). Salient features of our findings include (a) thioether-directed atroposelective C–H functionalization, (b) construction of N–C axially chiral scaffolds in the absence of toxic oxidants, and (c) key mechanistic insights into the mode of enantio-induction by DFT calculations.

Results and discussion

We first chose *N*-arylindoles **1a** bearing a thiomethyl group as the model substrate for the synthesis of N–C axially chiral motifs (Schemes 2 and S1 in the ESI†). We selected $Pd(OAc)_2$ as the catalyst and air as the oxidant to test various chiral acids. Several *N*-protected amino acids were first probed in the presence of ethyl acrylate (**2a**) in nBu_2O at 65 °C for 24 h. **L1–L3** afforded product **3a** in moderate yield albeit without enantioselectivity control. Next, simple chiral phosphoric acid (CPA, **L4**) was examined but no enantioinduction was detected. To our delight, when H8-Binol CPA **L5** bearing 9-anthracenyl substituents was examined, product **3a** was obtained in 60% yield with 87% ee. Further optimization of CPAs **L6–L9** indicated that **L8** was superior, leading to excellent enantiocontrol of 97% ee. Overall, the optimized reaction conditions were viable with ligand **L8** under air in nBu_2O at 65 °C.

With the optimized reaction conditions in hand, we next explored the generality of the palladium-catalyzed N–C atroposelective olefination (Scheme 3). A broad range of alkenes **2** provided the desired products **3a–3n** with excellent enantioselectivity up to 99% ee. Acrylates with different groups were well compatible with the catalytic system (Scheme 3, **3a–3g**). Specially, benzyl acrylate (**2f**) afforded the desired olefinated products **3f** with 99% ee. Acrylamide provided the desired olefinated product heterobiaryl **3h** in 67% yield with 90% ee. The absolute configuration of **3h** was unanimously assigned by single-crystal X-ray diffraction analysis (CCDC 2144688†), featuring a *R* configuration. Styrenes were also suitable partners for this transformation under 1 atm of oxygen. The reaction of 4-methoxystyrene proceeded to give the olefinated products **3i** in 58% yield with 97% ee. Electron-deficient CF_3-substituted styrene delivered product **3j** with slightly reduced enantiocontrol of 89% ee. Next, a variety of *N*-arylindoles **1k–1n** were tested. Thioether DG bearing benzyl substituent was well compatible with this transformation (**3k**). Indole **1l** with an electron-

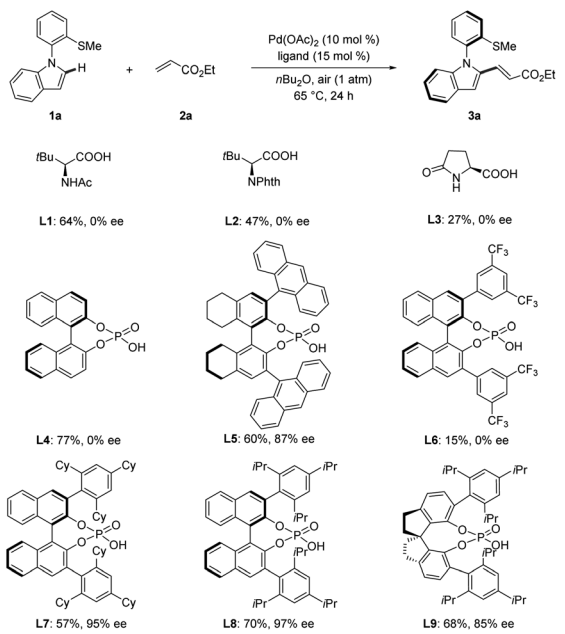

Scheme 2 Optimization of the N–C atroposelective C–H olefination. Reaction conditions: **1a** (0.10 mmol), **2a** (0.30 mmol), $Pd(OAc)_2$ (10 mol%), ligand (15 mol%), nBu_2O (2.0 mL), 65 °C, under air (1 atm). Yield was determined by ^1H NMR. The ee value was determined by HPLC analysis.

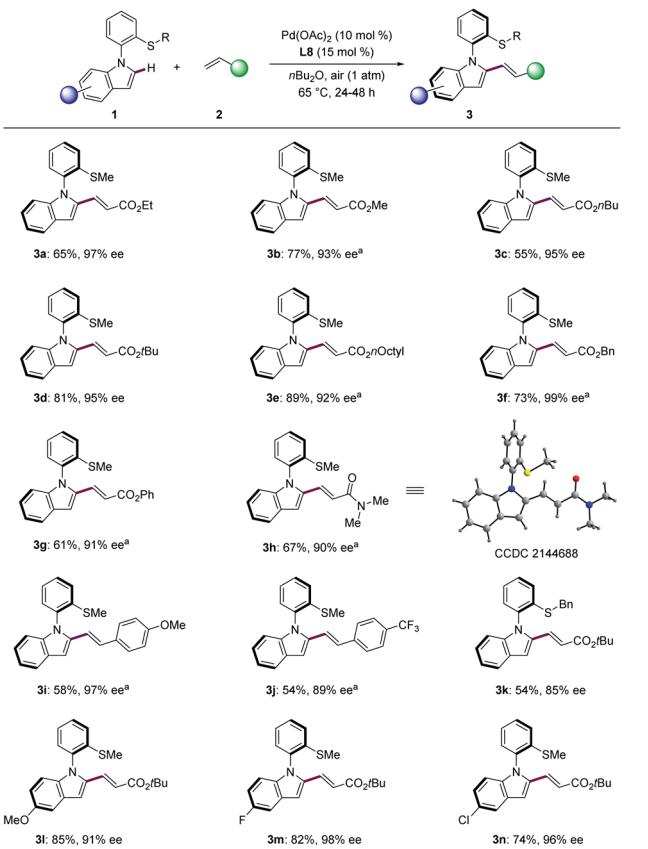

Scheme 3 N–C atroposelective C–H olefination of *N*-aryl indoles. [a] Under oxygen atmosphere.

donating methoxy group provided the corresponding olefinated product **3l** with 91% ee. The fluoro- and chloro-substituted indoles (**1m** and **1n**) were likewise tolerated in the N–C atropo-selective alkenylation with excellent enantioselectivity (**3m**, 98% ee; **3n**, 96% ee).

To further illustrate the diversity of the thioether-directed atroposelective C–H activation,[26] the construction of C–C axial chirality was next explored (Scheme 4). Various acrylates were well-tolerated with high enantiocontrol (**5a–5g**, 87–98% ee). When the aerobic olefination was performed on gram scale, the product **5c** was obtained in 86% yield and 98% ee. Acrylamide **2h** provided the desired olefinated product **5h** in 53% yield with 90% ee. In addition, the olefination with vinylphosphonate proceeded efficiently to give the product **5i** with excellent enantiocontrol (99% ee). High enantioselectivity (**5j**, 94% ee) was obtained when 4-methoxystyrene was employed as the olefination reagent. Next, we investigated the scope of biaryl thioethers. Biaryls with substituents on the naphthalene were well tolerated, giving the desired products (**5k**, 96% ee; **5l**, 95% ee). The absolute configuration of compound **5k** was assigned by single-crystal X-ray diffraction analysis (CCDC 2130699†), featuring a *R* configuration. In addition, substituted biaryls proved also feasible with enantioselectivity and furnished the corresponding products **5m–5o** with high ee. Substrates

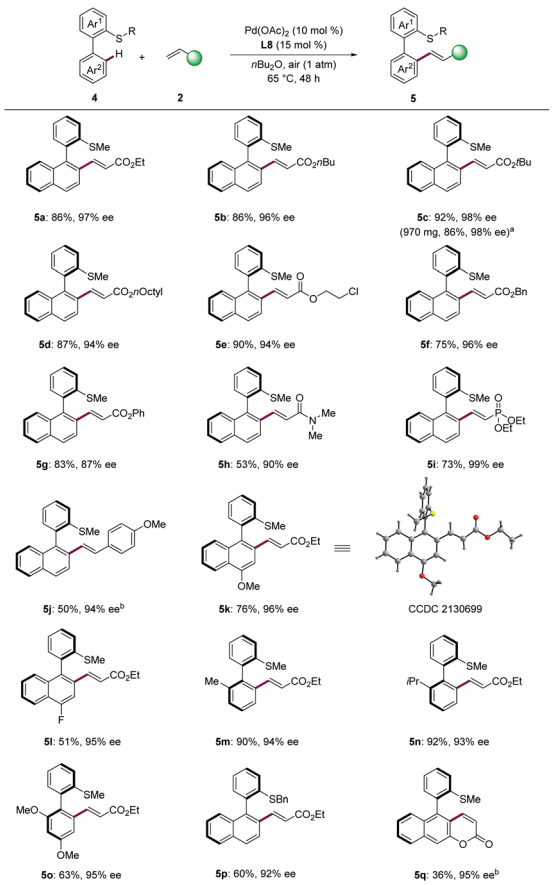

Scheme 4 C–C atroposelective C–H olefination of biaryls. [a] $Pd(OAc)_2$ (7.5 mol%), **L8** (12 mol%). [b] Under oxygen atmosphere.

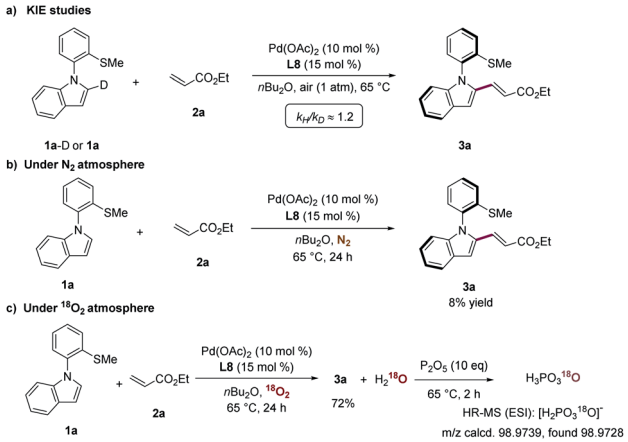

Scheme 5 Key mechanistic findings.

containing methoxy at the *ortho*- and *para*-position likewise gave the desired product **5o** in 63% yield with 95% ee. Thioether DGs bearing benzyl substituents was found compatible (**5p**, 60% yield, 92% ee). Interestingly, substrate with an acrylate substituent provided the desired intramolecular olefinated product **5q** with the coumarin scaffold in good enantioselectivity. This approach set the stage for the synthesis of coumarin scaffolds with axial chirality.

In order to shed light on the operative catalysis of this atroposelective C–H olefination, the kinetic isotope effect (KIE) experiment was performed by parallel reactions of substrates **1a**-D and **1a** with **2a** (Scheme 5a). The KIE of $k_H/k_D \approx 1.2$ was indicative of C–H activation not being the rate-determining step. Next, the reaction of substrates **1a** and **2a** under a nitrogen atmosphere provided product **3a** with a low yield of <10%, highlighting that catalytic turnover did not occur (Scheme 5b). The reaction under an atmosphere of isotopically-labeled $^{18}O_2$ atmosphere led to the selective formation of $H_2{}^{18}O$, which was trapped by P_2O_5 to afford the ^{18}O-containing phosphoric acid (Scheme 5c). These control experiments clearly showed that oxygen in the air was the oxidant for this aerobic transformation.

To gain insights into the N–C atroposelective C–H alkenylation, the reaction mechanism was probed by means of DFT calculations.[27] Free energy changes for the generation of *R*-configuration and *S*-configuration product are depicted in Fig. 1 and 2. Starting from the complexation of **L8** to $Pd(OAc)_2$ and the coordination of **1a**, intermediate **int1-R** is formed. Subsequently, **int1-R** undergoes a facile C–H activation step to form the arylpalladium species **int3-R**. This relatively low C–H activation barrier is consistent with the experimental KIE of 1.2 (Scheme 5a). The alkene coordination and the following insertion through **TS5-R** generates the alkylpalladium intermediate **int6-R**. Then, **int6-R** undergoes a β-hydride elimination to form a palladium hydride species **int8-R**, leading to the reduced palladium(0) complex **int10-R** with product coordination. Based on the most favorable pathway for the palladium-catalyzed N–C atroposelective C–H alkenylation, the rate-determining step is the β-hydride elimination, with a barrier of 21.6 kcal mol^{-1}. As

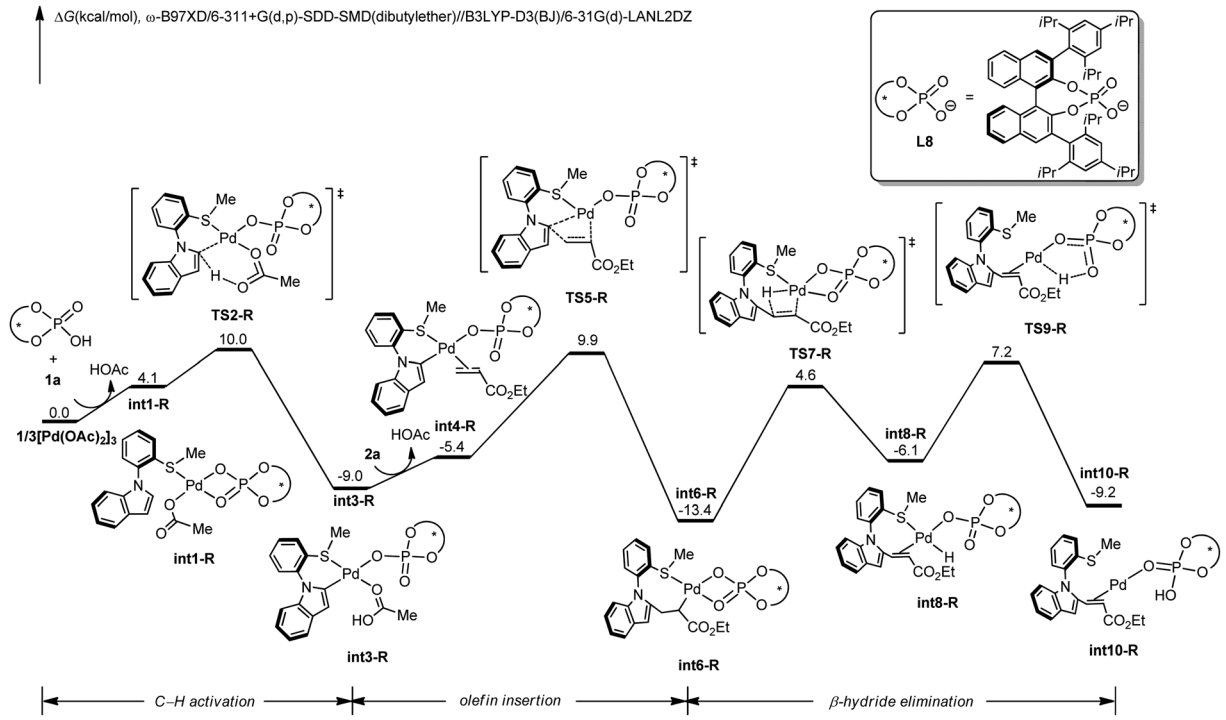

Fig. 1 DFT-computed free energy profile of palladium-catalyzed N–C atroposelective C–H alkenylation for *R*-enantiomer. Computational methods: ω-B97XD/6-311+G(d,p)-SDD-SMD(dibutylether)//B3LYP-D3(BJ)/6-31G(d)-LANL2DZ.

for the *S*-enantiomer, the initial C–H activation step is also facile. However, the olefin insertion step requires a barrier of 24.5 kcal mol^{-1}, which is significantly higher than the barrier for the *R*-enantiomer. Likewise, we also confirmed that the racemization of the axial chirality of the alkylpalladium intermediate **int6-R** is not feasible after the olefin insertion step

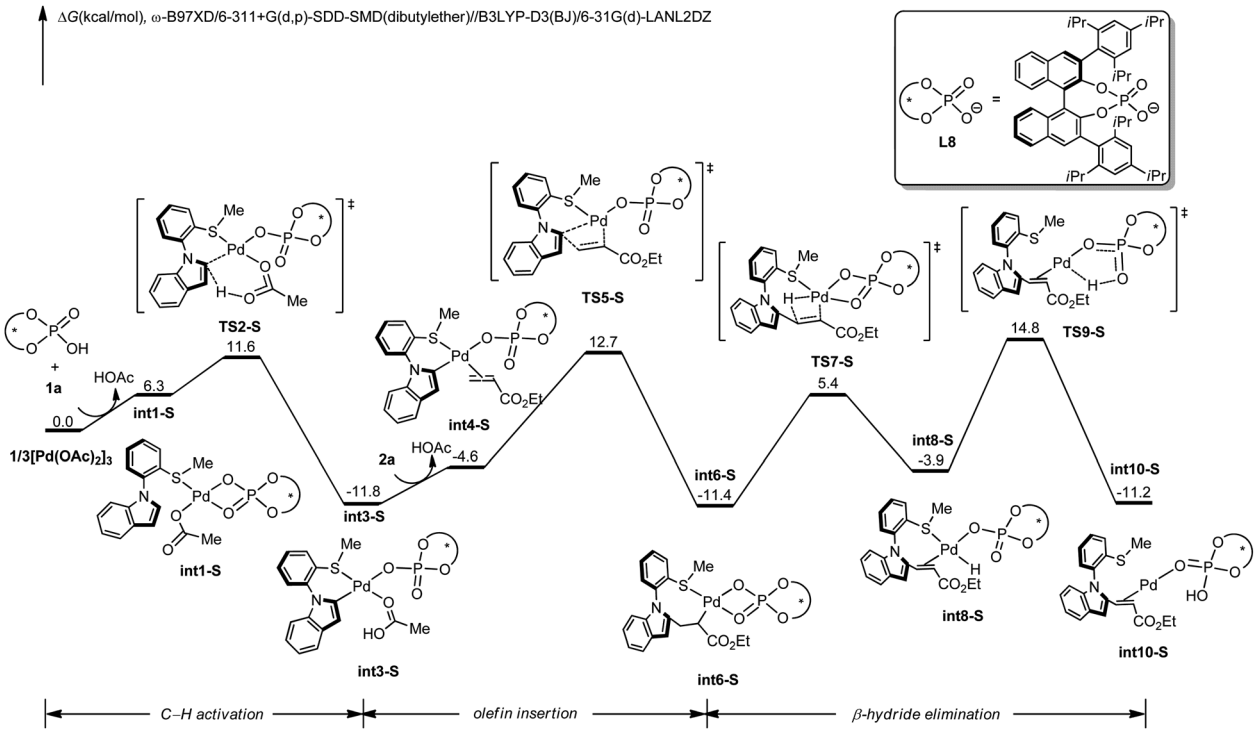

Fig. 2 DFT-computed free energy profile of palladium-catalyzed N–C atroposelective C–H alkenylation for *S*-enantiomer. Computational methods: ω-B97XD/6-311+G(d,p)-SDD-SMD(dibutylether)//B3LYP-D3(BJ)/6-31G(d)-LANL2DZ.

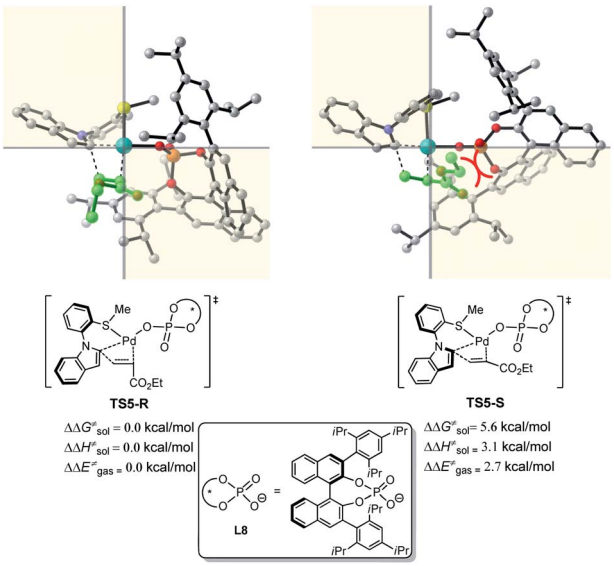

Fig. 3 DFT computed transition states involved in the enantioselectivity-determining step (olefin migratory insertion). In the transition state structures, non-participating hydrogens are removed for clarity.

(Fig. S3 in ESI†). Thereby, the olefin insertion is identified as the enantioselectivity-determining step.

To reveal the exact origins of enantioselectivity, we directed our attention to the nature of the migratory insertion transition states. Fig. 3 displays the optimized structures and relative free energies of the two competing enantioselectivity-determining transition states **TS5-R** and **TS5-S**. Thus, when comparing the two competitive transition states, the sterically demanding **L8** occupies the first and fourth quadrants. The substrate **1a** is in similar positions in the two transition states (second quadrant). The olefin **2a** (highlighted in green), however, is positioned in different quadrants. In the favoured transition state **TS5-R**, the ester group is in the third quadrant, which is distant from the bulky **L8**. In the disfavoured transition state **TS5-S**, the same ester group is positioned in the fourth quadrant, which leads to steric repulsions with the sterically congested ligand **L8**, being responsible for the destabilization of such transition state.

To evaluate the atropostability of the N–C axially chiral and the C–C axially chiral compounds, the rotational barriers and half-lifes for racemization of **3a** and **5a** were determined as depicted in Scheme 6. The results suggest that the C–C axially chiral compound **5a** is more atropostable than N–C axially chiral compound **3a**.

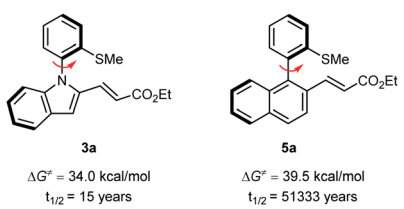

Scheme 6 Calculated rotational barriers for the racemization of products **3a** and **5a** and the corresponding half-life at 65 °C.

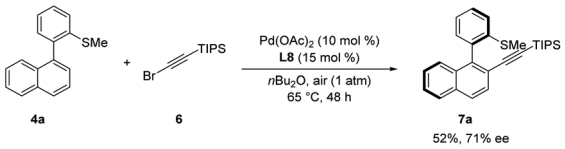

Scheme 7 Atroposelective palladium-catalyzed C–H alkynylation.

Encouraged by our results, we wondered whether the thioether-directed palladium-catalyzed atroposelective C–H functionalization might enable C–H alkynylation to prepare chiral molecules containing an alkynyl moiety. To our delight, and otherwise identical reaction conditions as the atroposelective C–H olefination, the reaction of biaryl substrate **4a** and TIPS protected alkynyl bromide **6** afforded product **7a** in 52% yield with moderate enantioselectivity (71% ee, Scheme 7).

Conclusion

In summary, we have reported on thioether-enabled atroposelective C–H olefination *via* a palladium/chiral phosphoric acid catalytic system. Both N–C and C–C axial chiralities were successfully established, leading to a broad range of axially chiral *N*-aryl indoles and biaryls with excellent enantioselectivities up to 99% ee. Notably, the catalytic system used air as the terminal oxidant instead of environmentally-unfriendly and expensive silver salts. Experimental and computational studies were conducted to illuminate the mechanism, which involves C–H activation, olefin insertion, and β-hydride elimination. The chiral induction mode of the enantioselectivity-determining step was identified by detailed DFT calculations.

Data availability

All experimental data, procedures for data analysis and pertinent data sets are provided in the ESI.†

Author contributions

Y. L. and L. A. conceived the project. Y. L. and Y.-C. L. performed the experiments, analyzed and interpreted the experimental data. X. C. performed DFT calculations. Y. L. and L. A. wrote the manuscript. All of the authors discussed the results and contributed to the preparation of the final manuscript.

Conflicts of interest

There are no conflicts to declare.

Acknowledgements

The authors gratefully acknowledge support from the ERC Advanced Grant no. 101021358, the DFG Gottfried-WilhelmLeibniz award (L. A.), and the Ministry of Science and Technology, Taiwan (scholarship 110-2917-I-003-002 to Y.-C. L.) The authors thank Dr Christopher Golz (University of Göttingen) for assistance with the X-ray diffraction analysis.

Notes and references

1 (*a*) J. E. Smyth, N. M. Butler and P. A. Keller, *Nat. Prod. Rep.*, 2015, **32**, 1562–1583; (*b*) A. Zask, J. Murphy and G. A. Ellestad, *Chirality*, 2013, **25**, 265–274.

2 (*a*) Q. Wang, Q. Gu and S.-L. You, *Angew. Chem., Int. Ed.*, 2019, **58**, 6818–6825; (*b*) C. Min and D. Seidel, *Chem. Soc. Rev.*, 2017, **46**, 5889–5902; (*c*) J. Yu, F. Shi and L.-Z. Gong, *Acc. Chem. Res.*, 2011, **44**, 1156–1171; (*d*) D. Parmar, E. Sugiono, S. Raja and M. Rueping, *Chem. Rev.*, 2014, **114**, 9047–9513; (*e*) T. Akiyama, J. Itoh and K. Fuchibe, *Adv. Synth. Catal.*, 2006, **348**, 999–1010.

3 (*a*) J. K. Cheng, S.-H. Xiang, S. Li, L. Ye and B. Tan, *Chem. Rev.*, 2021, **121**, 4805–4902; (*b*) T. Akiyama and K. Mori, *Chem. Rev.*, 2015, **115**, 9277–9306; (*c*) M. P. Carroll and P. J. Guiry, *Chem. Soc. Rev.*, 2014, **43**, 819–833; (*d*) Q.-L. Zhou, *Privileged Chiral Ligands and Catalysts*, Wiley-VCH, Weinheim, Germany, 2011; (*e*) J. F. Teichert and B. L. Feringa, *Angew. Chem., Int. Ed.*, 2010, **49**, 2486–2528; (*f*) W. Tang and X. Zhang, *Chem. Rev.*, 2003, **103**, 3029–3070; (*g*) Y. Chen, S. Yekta and A. K. Yudin, *Chem. Rev.*, 2003, **103**, 3155–3212; (*h*) R. Noyori and H. Takaya, *Acc. Chem. Res.*, 1990, **23**, 345–350.

4 J. Clayden, W. J. Moran, P. J. Edwards and S. R. LaPlante, *Angew. Chem., Int. Ed.*, 2009, **48**, 6398–6401.

5 Selected references:(*a*) Q.-H. Nguyen, S.-M. Guo, T. Royal, O. Baudoin and N. Cramer, *J. Am. Chem. Soc.*, 2020, **142**, 2161–2167; (*b*) Z.-J. Cai, C.-X. Liu, Q. Gu, C. Zheng and S.-L. You, *Angew. Chem., Int. Ed.*, 2019, **58**, 2149–2153; (*c*) S. Jerhaoui, J.-P. Djukic, J. Wencel-Delord and F. Colobert, *ACS Catal.*, 2019, **9**, 2532–2542; (*d*) J. Loup, V. Mgller, D. Ghorai and L. Ackermann, *Angew. Chem., Int. Ed.*, 2019, **58**, 1749–1753; (*e*) K. Liao, T. C. Pickel, V. Boyarskikh, J. Bacsa, D. G. Musaev and H. M. L. Davies, *Nature*, 2017, **551**, 609–613; (*f*) C.-J. Yoo, D. Rackl, W. Liu, C. B. Hoyt, B. Pimentel, R. P. Lively, H. M. L. Davies and C. W. Jones, *Angew. Chem., Int. Ed.*, 2018, **57**, 10923–10927; (*g*) J. Loup, D. Zell, J. C. A. Oliveira, H. Keil, D. Stalke and L. Ackermann, *Angew. Chem., Int. Ed.*, 2017, **56**, 14197–14201, for reviews:; (*h*) J. Loup, U. Dhawa, F. Pesciaioli, J. Wencel-Delord and L. Ackermann, *Angew. Chem., Int. Ed.*, 2019, **58**, 12803–12818; (*i*) T. G. Saint-Denis, R.-Y. Zhu, G. Chen, Q.-F. Wu and J.-Q. Yu, *Science*, 2018, **359**, eaao4798; (*j*) C. G. Newton, S.-G. Wang, C. C. Oliveira and N. Cramer, *Chem. Rev.*, 2017, **117**, 8908–8976; (*k*) J. Wencel-Delord and F. Colobert, *Chem.–Eur. J.*, 2013, **19**, 14010–14017.

6 (*a*) C.-X. Liu, W.-W. Zhang, S.-Y. Yin, Q. Gu and S.-L. You, *J. Am. Chem. Soc.*, 2021, **143**, 14025–14040; (*b*) J. Wencel-Delord, A. Panossian, F. R. Leroux and F. Colobert, *Chem. Soc. Rev.*, 2015, **44**, 3418–3430.

7 Selected references:(*a*) N. Jacob, Y. Zaid, J. C. A. Oliveira, L. Ackermann and J. Wencel-Delord, *J. Am. Chem. Soc.*, 2022, **144**, 798–806; (*b*) C.-Q. Pan, S.-Y. Yin, S.-B. Wang, Q. Gu and S.-L. You, *Angew. Chem., Int. Ed.*, 2021, **60**, 15510–15516; (*c*) C. Yang, T.-R. Wu, Y. Li, B.-B. Wu, R.-X. Jin, D.-D. Hu, Y.-B. Li, K.-J. Bian and X.-S. Wang, *Chem. Sci.*, 2021, **12**, 3726–3732; (*d*) L. Jin, Q.-J. Yao, P.-P. Xie, Y. Li, B.-B. Zhan, Y.-Q. Han, X. Hong and B.-F. Shi, *Chem*, 2020, **6**, 497–511; (*e*) Q. Wang, W.-W. Zhang, H. Song, J. Wang, C. Zheng, Q. Gu and S.-L. You, *J. Am. Chem. Soc.*, 2020, **142**, 15678–15685; (*f*) S. Shaaban, H. Li, F. Otte, C. Strohmann, A. P. Antonchick and H. Waldmann, *Org. Lett.*, 2020, **22**, 9199–9202; (*g*) Q.-H. Nguyen, S.-M. Guo, T. Royal, O. Baudoin and N. Cramer, *J. Am. Chem. Soc.*, 2020, **142**, 2161–2167; (*h*) Z.-S. Liu, Y. Hua, Q. Gao, Y. Ma, H. Tang, Y. Shang, H.-G. Cheng and Q. Zhou, *Nat. Catal.*, 2020, **3**, 727–733; (*i*) M. Tian, D. Bai, G. Zheng, J. Chang and X. Li, *J. Am. Chem. Soc.*, 2019, **141**, 9527–9532; (*j*) Q. Wang, Z.-J. Cai, C.-X. Liu, Q. Gu and S.-L. You, *J. Am. Chem. Soc.*, 2019, **141**, 9504–9510; (*k*) G. Shan, J. Flegel, H. Li, C. Merten, S. Ziegler, A. P. Antonchick and H. Waldmann, *Angew. Chem., Int. Ed.*, 2018, **57**, 14250–14254; (*l*) C. G. Newton, E. Braconi, J. Kuziola, M. D. Wodrich and N. Cramer, *Angew. Chem., Int. Ed.*, 2018, **57**, 11040–11210; (*m*) Y.-S. Jang, Ł. Woźniak, J. Pedroni and N. Cramer, *Angew. Chem., Int. Ed.*, 2018, **57**, 12901–12905; (*n*) C. He, M. Hou, Z. Zhu and Z. Gu, *ACS Catal.*, 2017, **7**, 5316–5320; (*o*) J. Zheng, W.-J. Cui, C. Zheng and S.-L. You, *J. Am. Chem. Soc.*, 2016, **138**, 5242–5245; (*p*) T. Wesch, F. R. Leroux and F. Colobert, *Adv. Synth. Catal.*, 2013, **355**, 2139–2144; (*q*) K. Yamaguchi, H. Kondo, J. Yamaguchi and K. Itami, *Chem. Sci.*, 2013, **4**, 3753–3757; (*r*) K. Yamaguchi, J. Yamaguchi, A. Studer and K. Itami, *Chem. Sci.*, 2012, **3**, 2165–2169.

8 G. Liao, T. Zhou, Q.-J. Yao and B.-F. Shi, *Chem. Commun.*, 2019, **55**, 8514–8523.

9 F. Kakiuchi, P. L. Gendre, A. Yamada, H. Ohtaki and S. Murai, *Tetrahedron: Asymmetry*, 2000, **11**, 2647–2651.

10 (*a*) J. Zheng and S.-L. You, *Angew. Chem., Int. Ed.*, 2014, **53**, 13244–13247; (*b*) D.-W. Gao, Q. Gu and S.-L. You, *ACS Catal.*, 2014, **4**, 2741–2745.

11 A. Romero-Arenas, V. Hornillos, J. Iglesias-Sigüenza, R. Fernandez, J. Lopez-Serrano, A. Ros and J. M. Lassaletta, *J. Am. Chem. Soc.*, 2020, **142**, 2628–2639.

12 (*a*) Q. Djerassi, J.-P. Jokic, J. Wencel-Delord and F. Colobert, *Angew. Chem., Int. Ed.*, 2018, **57**, 4668–4672; (*b*) Q. Dherbassy, G. Schwertz, M. Chessé, C. K. Hazra, J. Wencel-Delord and F. Colobert, *Chem.–Eur. J.*, 2016, **22**, 1735–1743; (*c*) C. K. Hazra, Q. Dherbassy, J. Wencel-Delord and F. Colobert, *Angew. Chem., Int. Ed.*, 2014, **53**, 13871–13875.

13 (*a*) S.-X. Li, Y.-N. Ma and S.-D. Yang, *Org. Lett.*, 2017, **19**, 1842–1845; (*b*) Y.-N. Ma, H.-Y. Zhang and S.-D. Yang, *Org. Lett.*, 2015, **17**, 2034–2037.

14 (*a*) B.-B. Zhan, L. Wang, J. Luo, X.-F. Lin and B.-F. Shi, *Angew. Chem., Int. Ed.*, 2020, **59**, 3568–3572; (*b*) B.-B. Zhan, Z.-S. Jia, J. Luo, L. Jin, X.-F. Lin and B.-F. Shi, *Org. Lett.*, 2020, **22**, 9693–9698; (*c*) J. Luo, T. Zhang, L. Wang, G. Liao, Q.-J. Yao, Y.-J. Wu, B.-B. Zhan, Y. Lan, X.-F. Lin and B.-F. Shi, *Angew. Chem., Int. Ed.*, 2019, **58**, 6708–6712.

15 (*a*) H.-M. Chen, G. Liao, C.-K. Xu, Q.-J. Yao, S. Zhang and B.-F. Shi, *CCS Chem.*, 2021, **3**, 455–465; (*b*) G. Liao, T. Zhang, Z.-K. Lin and B.-F. Shi, *Angew. Chem., Int. Ed.*,

2020, **59**, 19773–19786; (*c*) H. Song, Y. Li, Q.-J. Yao, L. Jin, L. Liu, Y.-H. Liu and B.-F. Shi, *Angew. Chem., Int. Ed.*, 2020, **59**, 6576–6580; (*d*) G. Liao, H.-M. Chen, Y.-N. Xia, B. Li, Q.-J. Yao and B.-F. Shi, *Angew. Chem., Int. Ed.*, 2019, **58**, 11464–11468; (*e*) J. Fan, Q.-J. Yao, Y.-H. Liu, G. Liao, S. Zhang and B.-F. Shi, *Org. Lett.*, 2019, **21**, 3352–3356; (*f*) G. Liao, Q.-J. Yao, Z.-Z. Zhang, Y.-J. Wu, D.-Y. Huang and B.-F. Shi, *Angew. Chem., Int. Ed.*, 2018, **57**, 3661–3665; (*g*) G. Liao, B. Li, H.-M. Chen, Q.-J. Yao, Y.-N. Xia, J. Luo and B.-F. Shi, *Angew. Chem., Int. Ed.*, 2018, **57**, 17151–17155; (*h*) Q.-J. Yao, S. Zhang, B.-B. Zhan and B.-F. Shi, *Angew. Chem., Int. Ed.*, 2017, **56**, 6617–6621.

16 T. Sugane, T. Tobe, W. Hamaguchi, I. Shimada, K. Maeno, J. Miyata, T. Suzuki, T. Kimizuka, S. Sakamoto and S.-i. Tsukamoto, *J. Med. Chem.*, 2013, **56**, 5744–5756.

17 (*a*) Y.-J. Wu, G. Liao and B.-F. Shi, *Green Synth. Catal.*, 2022, DOI: 10.1016/j.gresc.2021.12; (*b*) O. Kitagawa, *Acc. Chem. Res.*, 2021, **54**, 719–730.

18 (*a*) O. Kitagawa, *Acc. Chem. Res.*, 2021, **54**, 719–730; (*b*) A. Link and C. Sparr, *Chem. Soc. Rev.*, 2018, **47**, 3804–3815; (*c*) B. Zilate, A. Castrogiovanni and C. Sparr, *ACS Catal.*, 2018, **8**, 2981–2988; (*d*) D. Bonne and J. Rodriguez, *Chem. Commun.*, 2017, **53**, 12385–12393; (*e*) J. Wencel-Delord and F. Colobert, *Synthesis*, 2016, **48**, 2981–2996.

19 J. Frey, A. Malekafzali, I. Delso, S. Choppin, F. Colobert and J. Wencel-Delord, *Angew. Chem., Int. Ed.*, 2020, **59**, 8844–8848.

20 J. Zhang, Q. Xu, J. Wu, J. Fan and M. Xie, *Org. Lett.*, 2019, **21**, 6361–6365.

21 (*a*) Y.-J. Wu, Q.-J. Yao, X.-T. Xu, K. Zhang and B.-F. Shi, *Org. Lett.*, 2022, **24**, 304–308; (*b*) Y.-J. Wu, P.-P. Xie, G. Zhou, Q.-J. Yao, X. Hong and B.-F. Shi, *Chem. Sci.*, 2021, **12**, 9391–9397; (*c*) Q.-J. Yao, P.-P. Xie, Y.-J. Wu, Y.-L. Feng, M.-Y. Teng, X. Hong and B.-F. Shi, *J. Am. Chem. Soc.*, 2020, **142**, 18266–18276; (*d*) S. Zhang, Q.-J. Yao, G. Liao, X. Li, H. Li, H.-M. Chen, X. Hong and B.-F. Shi, *ACS Catal.*, 2019, **9**, 1956–1961.

22 (*a*) L. Sun, H. Chen, B. Liu, J. Chang, L. Kong, F. Wang, Y. Lan and X. Li, *Angew. Chem., Int. Ed.*, 2021, **60**, 8391–8395; (*b*) U. Dhawa, T. Wdowik, X. Hou, B. Yuan, J. C. A. Oliveira and L. Ackermann, *Chem. Sci.*, 2021, **12**, 14182–14188; (*c*) T. Li, C. Mou, P. Qi, X. Peng, S. Jiang, G. Hao, W. Xue, S. Yang, L. Hao, Y. R. Chi and Z. Jin, *Angew. Chem., Int. Ed.*, 2021, **60**, 9362–9367; (*d*) Z.-S. Liu, P.-P. Xie, Y. Hua, C. Wu, Y. Ma, J. Chen, H.-G. Cheng, X. Hong and Q. Zhou, *Chem*, 2021, **7**, 1917–1932; (*e*) U. Dhawa, C. Tian, T. Wdowik, J. C. A. Oliveira, J. Hao and L. Ackermann, *Angew. Chem., Int. Ed.*, 2020, **59**, 13451–13457; (*f*) W. Xia, Q.-J. An, S.-H. Xiang, S. Li, Y.-B. Wang and B. Tan, *Angew. Chem., Int. Ed.*, 2020, **59**, 6775–6779; (*g*) H. Li, X. Yan, J. Zhang, W. Guo, W. Jiang and J. Wang, *Angew. Chem., Int. Ed.*, 2019, **58**, 6732–6736; (*h*) M. E. Diener, A. J. Metrano, S. Kusano and S. J. Miller, *J. Am. Chem. Soc.*, 2015, **137**, 12369–12377.

23 (*a*) X.-S. Zhang, Q.-L. Zhu, Y.-F. Zhang, Y.-B. Li and Z.-S. Shi, *Chem.–Eur. J.*, 2013, **19**, 11898–11903; (*b*) J. Yao, M. Yu and Y. Zhang, *Adv. Synth. Catal.*, 2012, **354**, 3205–3210.

24 (*a*) L. Jin, P. Zhang, Y. Li, X. Yu and B.-F. Shi, *J. Am. Chem. Soc.*, 2021, **143**, 12335–12344; (*b*) T. G. Saint-Denis, N. Y. S. Lam, N. Chekshin, P. F. Richardson, J. S. Chen, J. Elleraas, K. D. Hesp, D. C. Schmitt, Y. Lian, C. W. Huh and J.-Q. Yu, *ACS Catal.*, 2021, **11**, 9738–9753.

25 (*a*) L. Ackermann, *Acc. Chem. Res.*, 2020, **53**, 84–104; (*b*) L. Ackermann, *Acc. Chem. Res.*, 2014, **47**, 281–295.

26 During the preparation of our manuscript, Shi and coworkers reported a study on the directing ability of chalcogenoethers in palladium-catalyzed atroposelective assembly of C–C axial chiral biaryls:G. Liao, T. Zhang, L. Jin, B.-J. Wang, C.-K. Xu, Y. Lan, Y. Zhao and B.-F. Shi, *Angew. Chem., Int. Ed.*, 2022, DOI: 10.1002/anie.202115221.

27 Computations were performed with the Gaussian 16 software package; computational details are included in the ESI†.